TRANSDUCER CALIBRATION IN TRANSMISSION ULTRASOUND COMPUTED TOMOGRAPHY

A. Filipík*, J. Jan*, R. Jiřík*, N. Ruiter**, and R. Stotzka**

* Brno University of Technology, Faculty of Electrical Engineering and Communication, Department of Biomedical Engineering, Brno, Czech Republic
** Forschungszentrum Karlsruhe, Institute of Data Processing and Electronics, Karlsruhe, Germany

xfilip10@stud.feec.vutbr.cz

Abstract: The paper presents a method for computing a frequency- and direction-dependent radiation function describing the properties of transducer elements in a transmission ultrasound computed tomography (USCT) system. Such a system consists of a water tank equipped with numerous unfocused ultrasonic transducer elements arranged on a plane circular perimeter of the tank. Each element may be used for emitting or receiving ultrasonic pulse waves that travel through and are scattered in the volume of the tank. USCT systems, still in development, are intended primarily for ultrasonic mammography and seem to be quite promising for this purpose. The presented method calculates a common directivity function and individual sensitivities of all transducer elements (in both, emitting and receiving modes). The calculation is based on solving a large set of log-linearized equations. At the end of this paper, it is shown that the model can be easily extended to include some apriori information about the USCT system.

Introduction

Ultrasonic Computed Tomography (USCT) is a relatively new imaging modality primarily aimed at breast cancer diagnosis. The examined object is placed in a water tank, equipped with several thousands of unfocused ultrasonic transducers. The scanning of the volume is done sequentially: at every step, one of the transducers emits an ultrasonic pulse and all of the other transducers are receiving the directly transmitted, scattered, and reflected waves (Figure 1). After the scanning is complete, a set of A-scans is obtained from which an image can be reconstructed using appropriate algorithms. Depending on the computation procedure, the spatial distribution of three different parameters of the scanned volume can be reconstructed: the ultrasonic reflectivity [1], the local ultrasonic attenuation [2], and the speed of the propagating ultrasound [3]. So far, these algorithms were based on simplified assumptions (omnidirectionality and equalized efficiency of the transducers), however, it is desirable to improve the reconstruction by including more realistic parameters of the transducers obtained by a calibration.

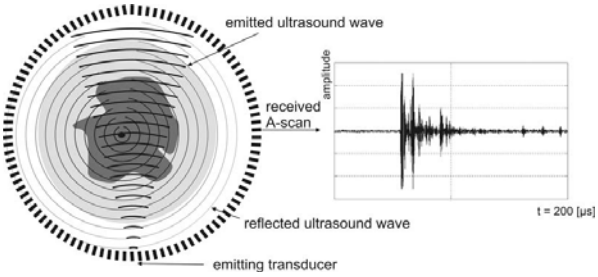

Figure 1: The USCT system. When one transducer is emitting, all the other transducers are receiving the transmitted, scattered, and reflected ultrasonic waves.

Although the used unfocused transducer elements are very small (<1mm), their directivity patterns are not ideally omnidirectional. These directivity patterns are also frequency dependent. It is thus possible to describe the transmitting/receiving properties of each transducer element by a two-dimensional angle and frequency dependent *radiation function*, which is the subject of measurement and calculation in the presented calibration method. Provided that the power of the emitted ultrasonic waves is low, we can assume linearity of the electro-acoustical transfer. It is thus possible to describe this 2D radiation function either by a set of 1D directivity patterns, each being valid for a different frequency, or by a set of 1D spectral transfer functions, each being valid for a certain emitting/receiving angle.

Materials and Methods

The calibration is based on a series of wide-band measurements with the tank filled only with water (so called “empty measurement”). Individual received signals (decomposed via DFT into frequency components) can be modeled as

$$S_{e,r}(f) \cong R_e(f,\vartheta_{e\to r}) \cdot R_r(f,\vartheta_{e\leftarrow r}) \tag{1}$$

where $S_{e,r}(f)$ is the amplitude spectrum of the received signal (using emitter *e* and receiver *r*), $R_e(f,\vartheta_{e\to r})$ is the radiation function of the emitter, $R_r(f,\vartheta_{e\leftarrow r})$ the radiation function of the receiver, *f* is frequency, $\vartheta_{e\to r}$ is the emitting angle (towards the receiver), and $\vartheta_{e\leftarrow r}$ is

ISSN: 1727-1983 © 2005 IFMBE

the receiving angle (towards the emitter) – see Figure 2. Taking each emitter – receiver – frequency combination, a system of equations can be constructed and log-linearized:

$$\log\left(S_{e,r}(f)\right) = \log\left(R_e(f, \vartheta_{e\to r})\right) + \log\left(R_r(f, \vartheta_{e\leftarrow r})\right), \forall e, r \quad (2)$$

Solution of this system provides the unknown parameters of the sensors. For N transducers with $N\text{-}1$ possible emitting/receiving angles and M frequency bands we are able to build $N \cdot (N-1) \cdot M$ equations with the same number of unknown parameters. Thus, it is theoretically possible to solve for an independent radiation function for each of the used transducers.

Given the limitations of the used experimental system, the measurements cannot provide a complete equation system. Only two movable ultrasonic probes simulate a 2D USCT ring of ultrasonic transducers surrounding the scanned volume. One of the probes is carrying an emitting transducer element, the other probe is carrying a linear array of 16 receiving transducer elements. Both move on a circular frame in 3.6° increments to simulate 100 emitters and 91x16 receivers (Figure 2).

For a certain position of the emitting transducer, the receiving probe is consecutively placed to the rest of the positions on the frame to record the transmitted ultrasonic waves. This way a "projection" of the scanned volume is made. This process is repeated for each emitting position to record the rest of the projections - similarly as in X-ray tomography.

Because only the empty measurements (USCT tank filled only with water) are used for the calibration, and the same (movable) set of transducers is used to make the whole set of projections, all of the projections should mutually contain the same information. Thus, all projections are linearly dependent, and by adding more projections, we are only making the solution more robust to noise (in the least mean squares sense).

For this experimental setup using $N_{e\text{-}pos}$ emitter probe positions (projections), 1 emitter transducer element, $N_{r\text{-}pos}$ receiver probe positions, $N_{r\text{-}el}$ receiver transducer elements, N_{freq} frequency bands, and N_{ang} emitting/receiving angles, we are able to build

$$N_{r-pos} \cdot N_{r-el} \cdot N_{freq} = 91 \cdot 16 \cdot 64 = 93184 \quad (3)$$

linearly independent equations, and

$$\begin{aligned}(1 + N_{r-el}) \cdot N_{freq} \cdot N_{ang} &= \\ = (1+16) \cdot 64 \cdot (16 \cdot 91) &= 1584128\end{aligned} \quad (4)$$

unknowns. As can be seen from these calculations, the system is greatly underdetermined and some simplifying assumptions are necessary to reduce the number of unknowns.

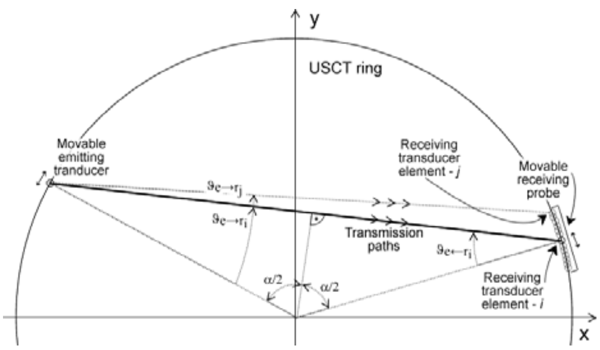

Figure 2: Geometry of the tomographic plane. The emitting transducer, receiving transducer and the center of the USCT ring form an equilateral triangle.

We can assume that all elements have a similar radiation function, because they are all manufactured equally and are of equal geometry. The minor differences caused by fatigue and material flaws may be represented by an individual multiplicative constant. We can call this constant *efficiency* (when the transducer is in emitting mode) or *sensitivity* (for the receiving mode), both supposedly equal (or rather linearly coupled). Thus, the radiation function of each transducer can be modeled by a product of a common 2D directivity function $D(f,\vartheta)$ and an individual sensitivity s (or efficiency e): $R(f,\vartheta) = s \cdot D(f,\vartheta)$.

As there are only 16 elements in the receiving probe of the experimental system, only 16 unknown sensitivities have to be determined. Because only one receiving transducer produces one measurement (e.g. one sensitivity value is present in one equation), there is no relation in the system between the sensitivity values of different transducer elements. This would give an infinite number of solutions to the system. However, if we don't insist on obtaining the absolute values of the transducer parameters, a relative solution can be defined by adding a suitable constraint to the system, e.g.:

$$\sum_{r-elements} \log\left(s_r\right) = 0 \quad (5)$$

which states, that the product of sensitivities s of all of the receiver elements will be equal to one.

A similar situation is with the efficiency of the emitting transducer. However, since there is only one transducer, which is gradually moved to all of the emitting positions, it contributes equally to every measurement. The efficiency may again be constrained a certain predefined value, in order to make the system solvable, e.g.:

$$\log(e) = 0, \quad (6)$$

i.e. the efficiency e of the emitting transducer is then equal to one. Nevertheless, these constraints only affect the absolute values of the solved parameters, not the important mutual relations. Moreover, the number of unknown quantities drops down dramatically:

ISSN: 1727-1983 © 2005 IFMBE

$$1 + N_{r-el} + N_{freq} \cdot N_{ang} = \\ = 1 + 16 + 64 \cdot (16 \cdot 91) = 93201. \quad (7)$$

To further decrease the number of unknowns, we can assume that the geometrical symmetry of each transducer element leads to a mirror symmetry of the directional characteristic in the image plane. Taking into account the scanning geometry (Figure 2), we can write:

$$D(f, \vartheta_{e \to r}) = D(f, \vartheta_{e \leftarrow r}) = D(f, \vartheta_{e \leftrightarrow r}). \quad (8)$$

Therefore, only a half of the directional coefficients needs to be calculated and the number of unknowns finally decreases bellow the number of equations:

$$1 + N_{r-el} + N_{freq} \cdot N_{ang} = \\ = 1 + 16 + 64 \cdot (16 \cdot 46) = 47121 \quad (9)$$

To make the system even more overdetermined we can make one final simplification. It is reasonable to assume a smooth change in the shape of the 2D directivity function along the angular axis. Then we can neglect the slight variation of the directivity function in the range of the 16 receiving elements (in a certain receiving and emitting arrangement) - see Figure 2:

$$D(f, \vartheta_{e \leftrightarrow r-el_1}) = D(f, \vartheta_{e \leftrightarrow r-el_2}) = ... = D(f, \vartheta_{e \leftrightarrow r}). \quad (10)$$

With this approximation, the number of unknowns further decreases significantly to:

$$1 + N_{r-el} + N_{freq} \cdot N_{ang} = \\ = 1 + 16 + 64 \cdot 46 = 2961 \quad (11)$$

Utilizing the above-mentioned assumptions in the log-linearized transmission signal model eq. (2), we arrive at the final equation system:

$$\log(S_{e,r}(f)) = \log(e) + \log(s) + 2 \cdot \log(D(f, \vartheta_{e \leftrightarrow r})), \forall e, r \quad (12)$$

Results

The proposed method was tested on the experimental 2D USCT system developed in Forschungszentrum Karlsruhe, Germany. The system is a simplified version of the generic one as described above: two ultrasonic probes (one carrying the emitting transducer and the other with a linear array of 16 receiving sensors) move on a circular frame to simulate all emitters and receivers. Transducers are approx. 0.22mm x 10mm (w x h), the pitch of the receiving array is 0.03 mm, and the diameter of the simulated USCT ring is about 120 mm.

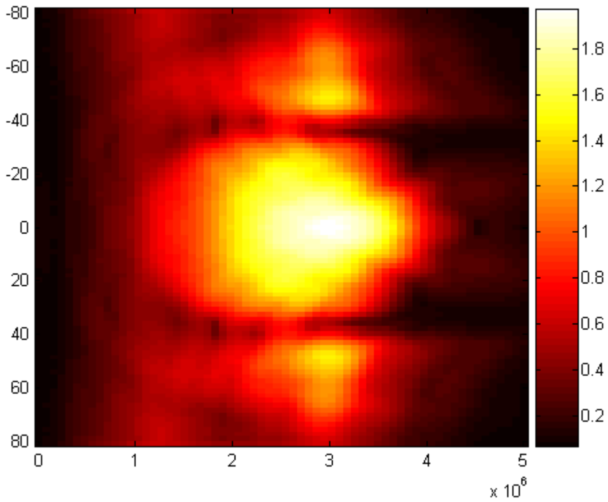

Figure 3: Obtained directivity function: vertical axis - emitting angle (degrees), horizontal axis - frequency (MHz)

Using data of the measurements in this geometry we have constructed a system of over 280 000 equations (using only 3 projections) with nearly 3 000 unknowns. The unknowns were solved for in the means of minimum square error using the singular value decomposition method [5]. An example of the common directivity function obtained this way is shown in Figure 3. The set of the relative efficiency coefficients for the receiving sensors is shown in Table 1.

Table 1: Calculated relative efficiencies of the receiving sensors (upper row: sensor number, lower row: sensitivity)

1	6	3	8	5	10	7
0.75	0.95	1.15	0.97	0.99	0.89	1.04

12	9	14	11	16	13	15
0.95	0.99	1.06	0.98	1.09	1.11	1.15

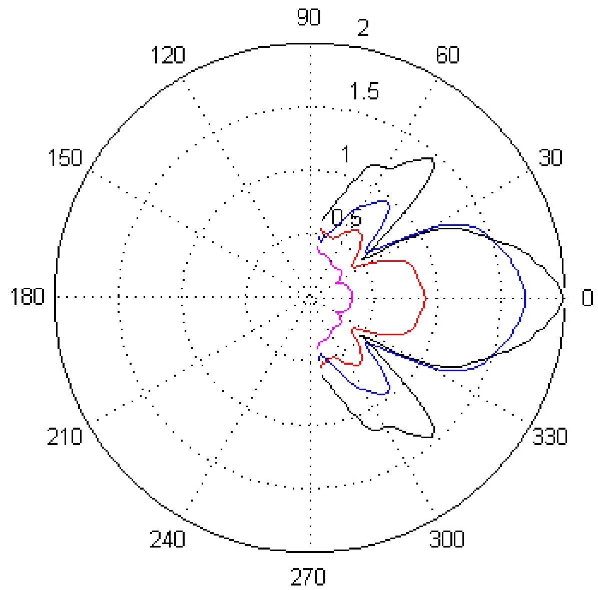

Figure 4: Angle dependency of the directivity function for different frequencies.

ISSN: 1727-1983 © 2005 IFMBE

In Figure 4 we can see normalized directivity patterns for different frequency bands (vertical slices of the 2D directivity function plotted in polar coordinates), whereas in Figure 5, spectral transfer functions for different emitting/receiving angles (horizontal slices of the 2D radiation function) are depicted.

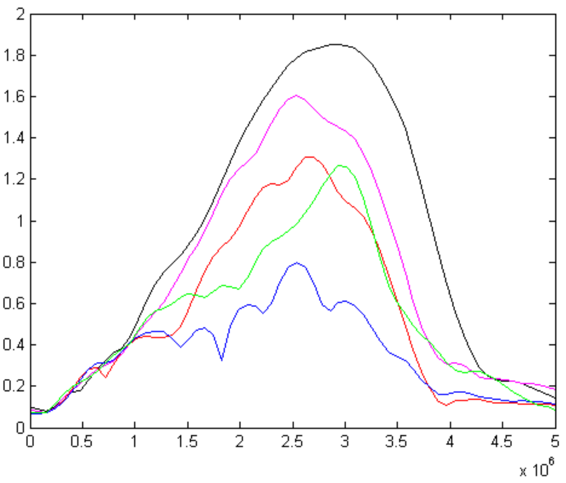

Figure 5: Frequency dependency of the directivity function at different angles. Horizontal axis: frequency (MHz).

Discussion

In order to verify the calculated results a set of measurements of the used transducers was taken. The emitted pressure field was measured with a hydrophone, along several semi arcs (in 5-degree steps) around the transducer at various distances [4]. Always the value of the highest peak of the received pulse was recorded. These values were then compared with the calculated values of the directivity function along the center frequency – cca. 2.9 MHz - (both functions were normalized to the highest value). As can be seen in Figure 6, these angular profiles show a reasonable correlation.

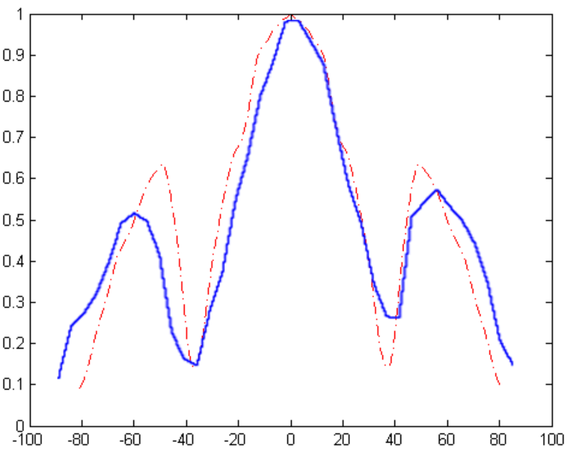

Figure 6: Comparison of angular characteristics. Solid - the pressure amplitude of the emitted field measured with a hydrophone. Dashed - computed directivity profile around the center frequency of the transducer.

In the above-described model used for transducer calibration, transfer functions of the electronics on the emitting and receiving sides were not considered. If there is a possibility to measure these, they can be easily included in the model. In addition, the attenuation of water and the distance between the emitting and receiving transducers can be taken into account to further increase the accuracy. The set of equations can then be written in the form of a product of several transfer functions:

$$S_{e,r}(f) = T_{ee} \cdot T_e \cdot T_w \cdot T_r \cdot T_{re}, \forall e, r, \tag{13}$$

where T_{ee} is the transfer function of the emitter electronics, T_e the transfer function of the emitting transducer (in the direction of the receiver), T_w the transfer function of the water path, T_r the transfer function of the receiving transducer (in the direction of the emitter), and T_{re} the transfer function of the receiving electronics. Using the above simplifications, we arrive at:

$$S_{e,r}(f) = T_{ee}(f) \cdot e \cdot s \cdot D^2\left(f, \vartheta_{e\leftrightarrow r}\right) \cdot e^{-\beta_w f l} \cdot T_{re}(f), \tag{14}$$

and its linearized version:

$$\begin{aligned} \log\left(S_{e,r}(f)\right) &= \log(e) + \log(s) + 2 \cdot \log(D(f, \vartheta_{e\leftrightarrow r})) + \\ &+ \log(T_{ee}(f)) + \log(T_{re}(f)) - (\beta_w + f + l), \forall e, r \end{aligned} \tag{15}$$

where β_w is the attenuation of water and l the length of the attenuation path. A further development in this direction is expected.

Conclusions

A method for calculating the (common) direction- and frequency-dependent directivity function and (individual) sensitivities of transducers in a transmission ultrasound computed tomography setup has been presented. The method was tested on data obtained by the experimental 2D USCT system developed in the Karlsruhe Forschungszentrum, Germany. The results are in reasonable agreement with the verifying measurements made by a hydrophone arrangement.

References

[1] STOTZKA, R., et al. (2002): 'Medical Imaging by Ultrasound-Computertomography', SPIE Medical Imaging, 2002/25.

[2] JIRIK R., STOTZKA R, TAXT T. (2005): 'Ultrasonic Attenuation Tomography Based on Log-Spectrum Analysis', Proceedings of SPIE, Medical Imaging 2005. Volume: 5750, pp. 305-314.

[3] MULLER, T.O. et al.: 'Ultrasound computertomography: image reconstruction using local absorption and sound speed profiles', ESEM - European Society for Engineering and Medicine, 2003.

[4] MING L. (2003): 'Ultrasound computertomography image reconstruction regarding object and sensor properties', Master thesis, Forschungszentrum Karlsruhe, University of Applied Science Karlsruhe, 2003.

[5] PRESS, W. H. et al. (2002): 'Numerical Recipes in C, The Art of Scientific Computing' (Second edition), Cambridge University Press, 2002.

ISSN: 1727-1983